


## Article

# Surfactants for Electrophoretic Deposition of Polyvinylidene Fluoride–Silica Composites

Zhengzheng Wang and Igor Zhitomirsky \* 

Department of Materials Science and Engineering, McMaster University, Hamilton, ON L8S4L7, Canada; wangz338@mcmaster.ca

\* Correspondence: zhitom@mcmaster.ca

**Abstract:** This investigation is motivated by the numerous advantages of electrophoretic deposition (EPD) for the fabrication of polyvinylidene fluoride (PVDF) and composite coatings and the various applications of such coatings. It is demonstrated that gallic acid (GA), caffeic acid (CFA), cholic acid (CA) and 2,3,4 trihydroxybenzoic acid (THB) can be used as charging and dispersing agents for the EPD of PVDF. The deposition yield of PVDF increases in the following order: THB < CFA < CA < GA. Test results indicate that the chemical structure of the dispersants exerts influence on the deposition efficiency. Potentiodynamic and impedance spectroscopy studies show the corrosion protection properties of PVDF coatings. GA is used for the co-EPD of PVDF with nanosilica and micron-size silica. The silica content in the composite coatings is varied by the variation of silica content in the suspensions. The ability to use GA as a charging and dispersing agent for the co-EPD of materials of different types paves the way for the fabrication of advanced organic–inorganic composites using EPD.

**Keywords:** polyvinylidene fluoride; silica; electrophoretic deposition; bile acid; catechol



**Citation:** Wang, Z.; Zhitomirsky, I. Surfactants for Electrophoretic Deposition of Polyvinylidene Fluoride–Silica Composites. *Surfaces* **2022**, *5*, 308–317. <https://doi.org/10.3390/surfaces5020022>

Academic Editor: Gaetano Granozzi

Received: 29 March 2022

Accepted: 10 May 2022

Published: 18 May 2022

**Publisher's Note:** MDPI stays neutral with regard to jurisdictional claims in published maps and institutional affiliations.



**Copyright:** © 2022 by the authors. Licensee MDPI, Basel, Switzerland. This article is an open access article distributed under the terms and conditions of the Creative Commons Attribution (CC BY) license (<https://creativecommons.org/licenses/by/4.0/>).

## 1. Introduction

Electrophoretic deposition (EPD) is an important technique for the surface modification of materials [1–3]. This technique is of particular interest for biomedical applications [4–7] due to the high purity of the deposited materials and the possibility of uniform deposition on complex shape substrates. Investigations focused on the development of advanced EPD bath formulations [8–10], particle charging additives [11], deposition kinetics and mechanisms [12–14]. Many investigations were performed on the EPD of organic–inorganic composites containing inorganic particles in a polymer matrix [4–6,15,16]. Significant interest has been generated in the use of biosurfactants for the fabrication of colloidal suspensions and the EPD of different materials [17–20]. The chemical structure of surfactants is an important factor controlling their adsorption on particles and the efficiency of particle dispersion [21–23]. A dispersant adsorbed on a particle's surface imparts an electric charge to the particles and allows for their electrophoretic transport to the electrode [24]. One of the challenges in the EPD technology is the charging, dispersion and deposition of chemically inert polymers. Another challenge is related to the co-deposition of such polymers with inorganic materials. Difficulties are related to the poor adsorption of traditional surfactants on the surfaces of such polymers and the selection of charged co-dispersants for the co-deposition of polymers with inorganic nanoparticles. However, there is a need in the development of EPD for the fabrication of composites, based on chemically inert advanced functional polymers, such as polyvinylidene fluoride (PVDF).

PVDF is a chemically inert polymer, which shows good resistance to inorganic and organic acids, various solvents and chemicals [25–27]. This polymer exhibits ferroelectric and piezoelectric properties, mechanical strength and low flammability [28–31]. Many PVDF applications involved the use of thin films and coatings [32–34]. Thin films were

used for piezoelectric actuators and transducers, pyroelectric sensors, electrical insulators and capacitors [28,35,36]. Significant interest has been generated in PVDF films for water treatment and the removal of pollutants, gas separation membranes, polymer fuel cells and batteries [37–40]. Of particular interest are PVDF applications in different biosensors [41–43]. PVDF films are under investigation for application in implantable biomedical devices [44–46]. PVDF and PVDF–silica composites have generated significant interest for biomedical tissue engineering [47–49].

PVDF was used as a binder for [50–53] the EPD of different materials. In this strategy, a small amount of dissolved PVDF was co-deposited with particles of inorganic or carbon materials. PVDF suspensions and solutions were used for EPD without charged dispersants [54–56]. However, the charging and deposition mechanisms were not understood. The EPD of PVDF films was achieved using bile acids as dispersing and charging agents [57].

This investigation was motivated by the need for the fabrication of PVDF and composite films and the numerous advantages of the EPD deposition method. The goal of this investigation was the EPD of pure PVDF and PVDF–silica films. The influence of different dispersants on the deposition yield was investigated. The highest deposition yield of PVDF was achieved using gallic acid (GA) as a dispersant. The PVDF films deposited using GA as a dispersant provided corrosion protection of stainless steel substrates. The use of GA facilitated the co-deposition of PVDF with micro- and nanosilica. The amount of silica co-deposited with PVDF could be varied. The results of this investigation indicated that catecholates and gallates can be used as efficient co-dispersants for the co-deposition of PVDF with inorganic particles.

## 2. Materials and Methods

Poly (vinylidene fluoride) (PVDF, spherical particles, diameter 100 nm, Alfa Aesar, Tewksbury, MA, USA), gallic acid (GA), caffeic acid (CFA), cholic acid (CA), 2,3,4 trihydroxybenzoic acid (THB), NaCl, nanosilica (size 5–20 nm, MilliporeSigma, Oakville, ON, Canada) and micron-size silica (size  $1 \mu\text{m} \pm 10\%$ , PCR Inc., Cumming, GA, USA) were used.

PVDF films were prepared via EPD from  $5 \text{ g L}^{-1}$  PVDF suspensions in ethanol, containing  $1 \text{ g L}^{-1}$  dispersants, such as GA, CFA, CA and THB. The dispersants were dissolved in ethanol, and then, PVDF particles were added. Ultrasonication was performed for 30 min in order to obtain stable suspensions for EPD. The EPD of composite films was performed from  $5 \text{ g L}^{-1}$  PVDF suspensions, containing  $1\text{--}8 \text{ g L}^{-1}$  silica particles and  $1\text{--}2 \text{ g L}^{-1}$  dispersants. Silica particles were added to the PVDF suspensions, containing dissolved dispersants. Ultrasonication was performed for 30 min for the fabrication of stable suspensions for EPD. A type 304 stainless steel (dimensions  $25 \times 30 \times 0.12 \text{ mm}$ ) functioned as the working electrode, while a platinum sheet (dimensions  $25 \times 30 \times 0.1 \text{ mm}$ ) acted as the counter electrode, with a 17 mm spacing between them in the EPD cell. An Amersham Biosciences EPS 2A200 power supply was used for EPD. EPD was performed for 1–5 min at a deposition voltage of 100 V between two electrodes. Following deposition, the coatings were dried at room temperature before being thermally treated in a Carbolite ELF furnace at  $200 \text{ }^\circ\text{C}$  for 1 h for further characterization. Deposition yield measurements were performed via measurement of substrate mass before and after deposition using precise Mettler Toledo XSR104 Analytical Balance.

Zeta potential measurements were performed by a mass transfer method [58]. FTIR studies were performed using a Bruker Vertex 70 spectrometer (USA). A PARSTAT 2273 potentiostat from Ametek (USA) was used to conduct electrochemical characterization of coated and uncoated substrates in a 3.0 wt% aqueous NaCl solution with a 3-electrode cell that included an uncoated or coated stainless steel substrate as a working electrode, a saturated calomel reference electrode (SCE), and a Pt mesh counter electrode. The testing technique and data analysis were both controlled by PowerSuite software. To reduce the influence of oxygen, the aqueous NaCl solution was deoxygenated for at least 30 min

using inert nitrogen gas before each test. Potentiodynamic polarization experiments were carried out at a  $1.0 \text{ mV s}^{-1}$  sweeping rate. Electrochemical impedance spectroscopy (EIS) experiments were carried out in the frequency range from 10 mHz to 10 kHz with a sinusoidal excitation voltage of 10 mV. Microstructure analysis was carried out using a JEOL JSM-7000F (Tokyo, Japan) scanning electron microscope (SEM) and a Talos 200X (ThermoFisher Scientific, Waltham, MA, USA) transmission electron microscope (TEM).

### 3. Results and Discussion

Figure 1 shows TEM images of PVDF particles used for EPD. The particles had a spherical shape with uniform diameters of  $\sim 200 \text{ nm}$ . PVDF is an electrically neutral polymer. Therefore, PVDF particles must be charged and dispersed using additives for film formation via EPD. Figure 2 shows structures of GA, CFA, CA and THB used in this investigation as additives for PVDF deposition.

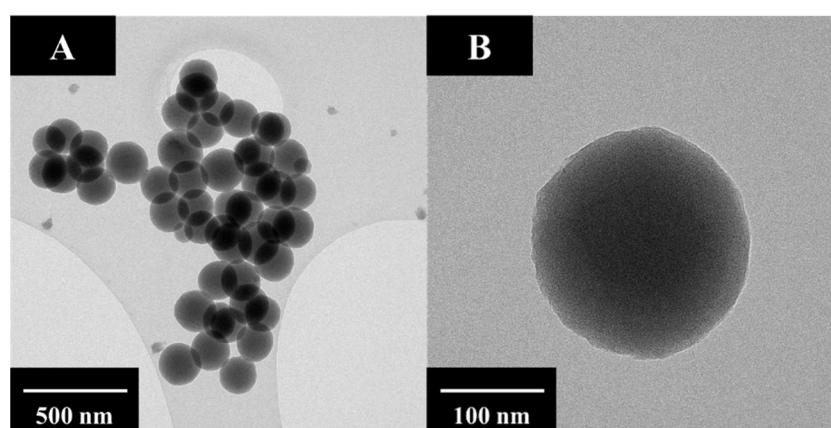


Figure 1. TEM images of PVDF particles at (A,B) different magnifications.

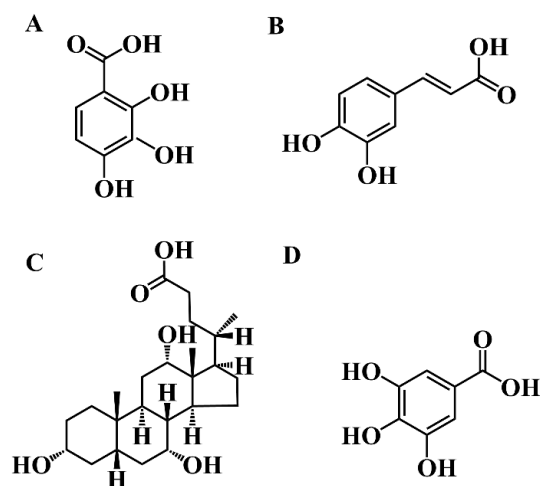


Figure 2. Chemical structures of (A) THB, (B) CFA, (C) CA and (D) GA.

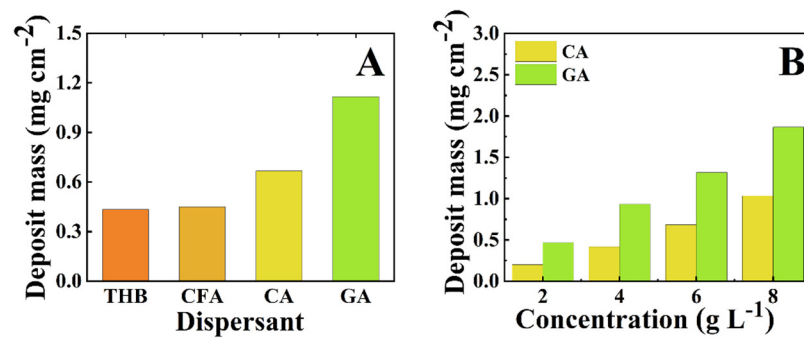
The chemical structures of GA, CFA, CA and THB contain anionic COOH groups. The chemical structures of CA and aromatic GA, CFA and THB molecules are beneficial for their adsorption on organic materials [19]. THB, CA and GA are especially attractive for adsorption on inorganic materials, because such molecules can be adsorbed on particle surfaces via catecholate-type bonding (GA, CFA and THB) or salicylate-type bonding (THB) [18]. The interest in gallates and catecholates for the EPD of metal oxides resulted from the analysis of strong catecholate-type bonding of mussel proteins to inorganic surfaces [59–61]. In previous investigations, aromatic catecholate- and gallate-type molecules containing COOH groups and salicylate-type molecules were used as charging and dispersing agents

for the anodic EPD of different oxide particles in ethanol [62–66]. The adsorption of catecholate molecules containing COOH groups on positively charged MnO<sub>2</sub> particles resulted in a charge reversal and allowed for the anodic deposition of MnO<sub>2</sub> films from particle suspensions in ethanol [67].

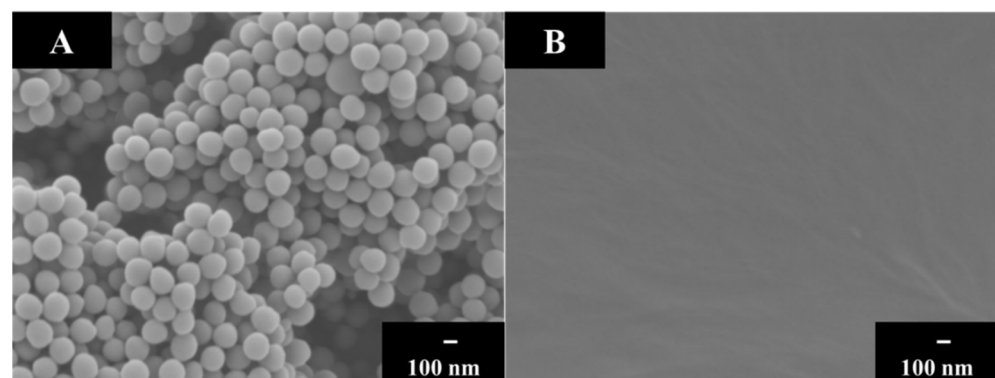
The addition of GA, CFA, CA and THB to the PVDF suspensions in ethanol allowed for the fabrication of PVDF films via EPD. The suspensions of electrically neutral PVDF were unstable, and EPD was not achieved from such suspensions. It was hypothesized that added dispersants adsorbed on PVDF particles imparted an electric charge to the particles and allowed for the suspension stabilization and deposition of PVDF from stable suspensions. Dispersant adsorption on particles can result from hydrophobic interactions. Figures 3B and S1 (Supplementary Materials) show the deposit masses of the films prepared with different dispersants at a PVDF concentration of 5 g L<sup>-1</sup>. The EPD experiments indicated that selected anionic dispersants adsorbed on the PVDF imparted charge to the PVDF particles and allowed their EPD. The chemical structures of the aromatic dispersants THB, CFA and GA exerted influence on the deposition efficiency, with the highest deposition yield obtained using GA. The deposition yield obtained using CA was higher than that obtained using THB and CFA. The deposition yield increased in the following order: THB < CFA < CA < GA. The suspensions containing CA and GA were further investigated due to the larger deposition yields obtained using such dispersants. Moreover, CA and GA are promising for the dispersion and charging of inorganic particles because they allow for catecholate-type bonding to the particle surface [18]. The deposition yield increased with increasing PVDF concentration in suspensions with the highest deposition yield achieved using GA for all PVDF concentrations (Figures 3B and S2). The deposition yield of PVDF increased with increasing deposition voltage and time (Figures S3 and S4). Zeta potentials of PVDF particles obtained in the presence of THB, CFA, CA and GA were found to be -4.2, -4.5, -7.1 and -13.9 mV, respectively. The highest deposition yield and zeta potential of PVDF achieved using GA indicated stronger GA adsorption on PVDF and enhanced particle charging. The EPD of PVDF was optimized using GA dispersant at the deposition voltage of 100 V, deposition time of 5 min and PVDF concentration of 5 g L<sup>-1</sup>. It should be noted that at higher voltages, deposition times and PVDF concentrations, the deposition process required the addition of a polymer binder due to increased deposit mass and risk of spalling of green deposits. A GA concentration of 1 g L<sup>-1</sup> was the minimum concentration required for EPD from 5 g L<sup>-1</sup> PVDF solutions and the co-EPD of PVDF with micron-size silica. It is shown below that in the case of nanosilica with smaller particle sizes and large nanosilica concentrations, the GA content could be increased to 2 g L<sup>-1</sup> in order to achieve the improved co-deposition of nanosilica with PVDF. The deposition of PVDF was also confirmed by results of Fourier Transform Infrared Spectroscopy (FTIR). The comparison of the FTIR spectrum of the as-received PVDF powder and spectra of deposits obtained using THB, CFA, CA and GA dispersants (Figure S5) indicated that PVDF coatings were deposited via EPD. The spectra of the deposits contained characteristic peaks of as-received PVDF (Figure S5).

Figure 4A shows SEM images of the as-deposited PVDF film. The as-deposited film was porous. Annealing at 200 °C for 1 h resulted in the PVDF melting and the formation of a dense film (Figure 4B).

The annealed PVDF films showed promising corrosion protection properties. Figure 5 presents potentiodynamic testing data for coated and uncoated substrates. Coated substrates showed a lower corrosion current of 0.27 μA cm<sup>-2</sup>, compared to the corrosion current of 2.6 μA cm<sup>-2</sup> for uncoated steel. The Tafel plot for the coated sample showed reduced anodic current and increased corrosion potential. Moreover, the Bode plots of impedance data confirmed corrosion protection properties of the PVDF coatings (Figure 6). Coated samples showed larger impedance compared to uncoated substrate in 3% NaCl solutions. Therefore, deposited coating provided a barrier preventing electrolyte access to the substrate.



**Figure 3.** (A) Deposit mass achieved for different dispersants using  $5 \text{ g L}^{-1}$  PVDF suspensions containing  $1 \text{ g L}^{-1}$  dispersants, (B) deposit mass versus PVDF concentration in suspensions, containing  $1 \text{ g L}^{-1}$  dispersants for deposition time of 5 min and deposition voltage of 100 V.



**Figure 4.** SEM images of (A) as-deposited and (B) annealed PVDF films fabricated via EPD from  $5 \text{ g L}^{-1}$  PVDF suspension containing  $1 \text{ g L}^{-1}$  GA as a dispersant. The films were obtained at deposition time of 5 min and deposition voltage of 100 V.

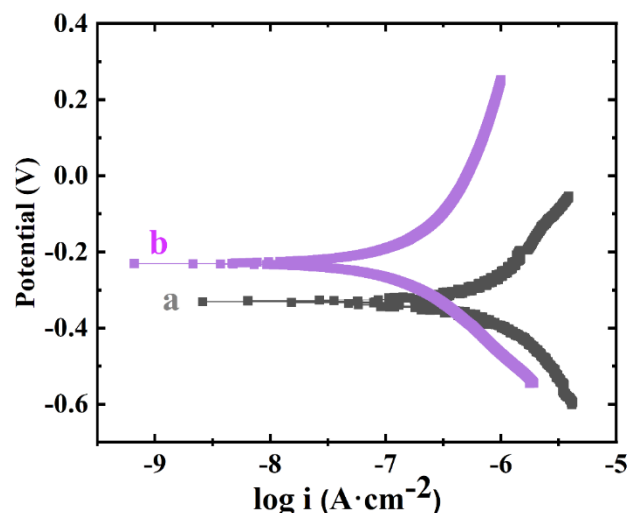


**Figure 5.** Tafel plots for (a) uncoated substrate and (b) coated from  $5 \text{ g L}^{-1}$  PVDF suspensions containing  $1 \text{ g L}^{-1}$  GA and annealed at  $200 \text{ }^\circ\text{C}$ . PVDF films were obtained at deposition time of 5 min and deposition voltage of 100 V.

As pointed out above, GA is an important dispersant for the EPD of oxide materials [18], which allows for catecholate-type bonding to metal atoms on the particle surface. Therefore, it was hypothesized that GA can act as a co-dispersant for PVDF and silica particles. The co-EPD of PVDF and silica was performed using micron-size silica and nanosilica. Figure 7 shows SEM images of coatings prepared from PVDF and silica particles and dispersed using GA. The SEM images at different magnifications showed crack-free coatings

containing nanosilica or micron-size silica particles. The particles were incorporated into the PVDF matrix as individual particles or agglomerates. The EPD of composite films was performed from suspensions with different concentrations of silica particles. Figure 8 shows films mass as a function of silica concentration in  $5 \text{ g L}^{-1}$  PVDF suspensions, containing  $1 \text{ g L}^{-1}$  GA. The deposition yield for suspensions, containing micron-size silica particles increased with increasing concentrations of particles in suspension. The increase in the deposition yield indicated the increased deposition of silica and the possibility of variations in coating composition. The deposition yield for suspensions containing nanosilica increased in the concentration range of  $0\text{--}4 \text{ g L}^{-1}$  and remained nearly constant at higher nanosilica concentrations. It is suggested that larger GA content is necessary for dispersion and deposition on nanosilica due to the larger surface area of this material. Indeed, a continuous increase in the deposition yield was observed with increasing nanosilica content in suspensions containing  $5 \text{ g L}^{-1}$  PVDF and  $2 \text{ g L}^{-1}$  GA (Figure S6). It is important to note that applications of many charging agents for EPD are limited to materials of specific types, such as metal oxides or carbon materials. The fabrication of composite coatings requires the use of advanced charging agents suitable for the charging of materials of different types. Therefore, GA is a promising charging agent for the fabrication of advanced organic–inorganic composites.

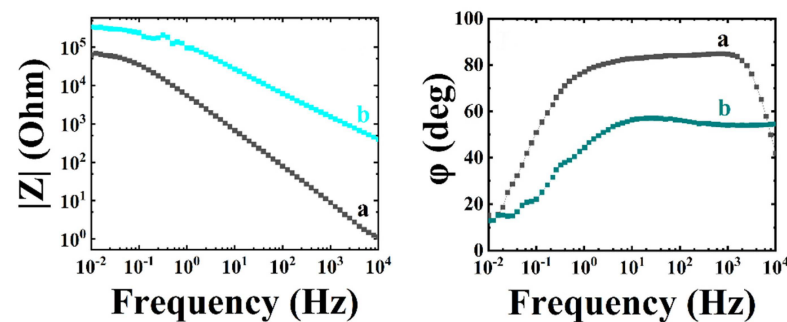


**Figure 6.** Bode plots for (a) uncoated substrate and (b) coated from  $5 \text{ g L}^{-1}$  PVDF suspensions containing  $1 \text{ g L}^{-1}$  GA and annealed at  $200 \text{ }^\circ\text{C}$ . PVDF films were obtained at deposition time of 5 min and deposition voltage of 100 V.

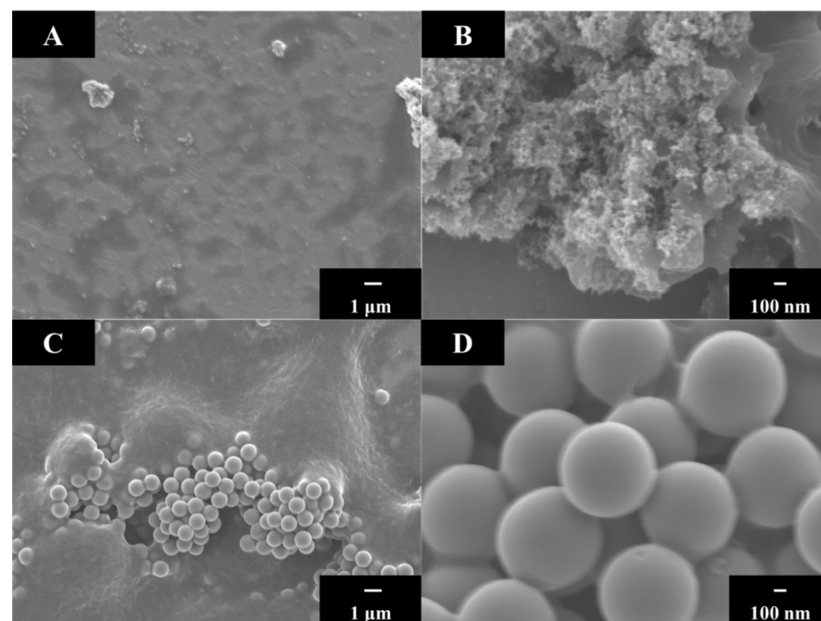


**Figure 7.** SEM images at different magnifications for coatings deposited from  $5 \text{ g L}^{-1}$  PVDF suspensions, containing  $1 \text{ g L}^{-1}$  GA and  $1 \text{ g L}^{-1}$  (A,B) nanosilica and (C,D) micron-size silica and annealed at  $200 \text{ }^\circ\text{C}$ . Deposition was performed during 5 min at a deposition voltage of 100 V.

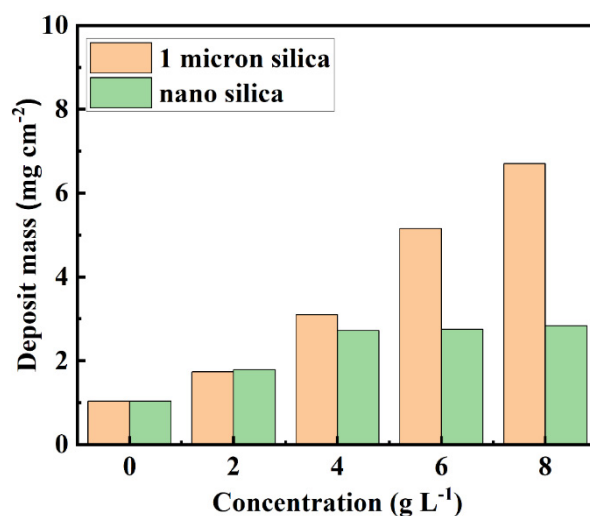


**Figure 8.** Deposit mass versus silica concentration in 5 g L<sup>-1</sup> PVDF suspension containing 1 g L<sup>-1</sup> GA. Deposition was performed during 5 min at a deposition voltage of 100 V.

The co-deposition of PVDF with nanosilica and micron-size silica was also confirmed via the comparison of SEM images of annealed pure PVDF films without silica and with nanosilica or micron-size silica (Figure S7).

EPD is a promising technique for the deposition of PVDF and composites based on the functional properties of PVDF and other functional materials. Such composites can potentially be used for applications in biomedical implants and devices. The results of this investigation pave the way for the deposition of PVDF films for applications based on the piezoelectric and ferroelectric properties of this polymer [68]. EPD is a versatile alternative for the fabrication of multifunctional composites, combining ferroelectric and magnetic properties of materials [69,70], thin film sensors [71], and energy storage devices [72].

#### 4. Conclusions

GA, CFA, CA and THB showed adsorption on chemically inert, electrically neutral PVDF particles and were used as charging and dispersing agents for the EPD of PVDF coatings. The deposition yield of PVDF increased in the following order: THB < CFA < CA < GA. PVDF coatings exhibited corrosion protection properties. GA can be used as a charging dispersant for the co-deposition of PVDF with nanosilica or micron-size silica and the fabrication of composite films. The film composition can be varied by the variation of silica concentration in suspensions for EPD. The use of GA as a charging co-dispersant for materials of different types paves the way for the deposition of advanced organic–inorganic composites.

**Supplementary Materials:** The following supporting information can be downloaded at: <https://www.mdpi.com/article/10.3390/surfaces5020022/s1>, Figure S1: Deposit mass achieved for different dispersants using 5 g L<sup>-1</sup> PVDF suspensions containing 1 g L<sup>-1</sup> dispersants for deposition time of 5 min and deposition voltage of 50 V; Figure S2: Deposit mass versus PVDF concentration in suspensions, containing 1 g L<sup>-1</sup> dispersants for deposition time of 5 min and deposition voltage of 50 V; Figure S3: Deposit mass versus deposition time at a deposition voltage of 100 V for 5 g L<sup>-1</sup> PVDF suspensions; Figure S4: Deposit mass versus deposition voltage for 5 g L<sup>-1</sup> PVDF suspensions at deposition time of 5 min; Figure S5: FTIR spectra of deposits, prepared from using 5 g L<sup>-1</sup> PVDF suspensions containing 1 g L<sup>-1</sup> dispersants: (a) THB, (b) CFA, (c) CA, (d) GA for deposition time of 5 min and deposition voltage of 100 V and (e) as-received PVDF; Figure S6: Deposit mass versus nanosilica concentration in 5 g L<sup>-1</sup> PVDF suspension containing 2 g L<sup>-1</sup> GA at deposition time of 5 min at voltages of 50 V and 100 V; Figure S7: SEM images of coatings, prepared from 5 g L<sup>-1</sup> PVDF solution, containing 1 g L<sup>-1</sup> GA (A) without silica, (B) with 1 g L<sup>-1</sup> nanosilica and (C) with 1 g L<sup>-1</sup> micron size silica deposited at a deposition voltage of 100 V and deposition time of 5 min and annealed at 200 °C for 1 h [73,74].

**Author Contributions:** Conceptualization, Z.W. and I.Z.; methodology, Z.W.; software, Z.W.; validation, Z.W. and I.Z.; formal analysis, Z.W. and I.Z.; investigation, Z.W.; resources, I.Z.; data curation, Z.W.; writing—original draft preparation, Z.W. and I.Z.; writing—review and editing, Z.W. and I.Z.; visualization, Z.W.; supervision, I.Z.; project administration, I.Z.; funding acquisition, I.Z. All authors have read and agreed to the published version of the manuscript.

**Funding:** This research was funded by the Natural Sciences and Engineering Research Council of Canada, grant number RGPIN-2018-04014, and the CRC program.

**Data Availability Statement:** Data is contained within the article or supplementary materials.

**Acknowledgments:** The authors acknowledge the support of the Natural Sciences and Engineering Research Council (NSERC) of Canada, the CRC program and the Canadian Centre for Electron Microscopy.

**Conflicts of Interest:** The authors declare no conflict of interest.

## References

1. Mishyn, V.; Aspermaier, P.; Leroux, Y.; Happy, H.; Knoll, W.; Boukherroub, R.; Szunerits, S. “Click” Chemistry on Gold Electrodes Modified with Reduced Graphene Oxide by Electrophoretic Deposition. *Surfaces* **2019**, *2*, 193–204. [[CrossRef](#)]
2. Besra, L.; Liu, M. A review on fundamentals and applications of electrophoretic deposition (EPD). *Prog. Mater. Sci.* **2007**, *52*, 1–61. [[CrossRef](#)]
3. Van der Biest, O.O.; Vandeperre, L.J. Electrophoretic deposition of materials. *Annu. Rev. Mater. Sci.* **1999**, *29*, 327–352. [[CrossRef](#)]
4. Batool, S.A.; Wadood, A.; Hussain, S.W.; Yasir, M.; Ur Rehman, M.A. A Brief Insight to the Electrophoretic Deposition of PEEK-, Chitosan-, Gelatin-, and Zein-Based Composite Coatings for Biomedical Applications: Recent Developments and Challenges. *Surfaces* **2021**, *4*, 205–239. [[CrossRef](#)]
5. Ahmed, Y.; Yasir, M.; Ur Rehman, M.A. Fabrication and Characterization of Zein/Hydroxyapatite Composite Coatings for Biomedical Applications. *Surfaces* **2020**, *3*, 237–250. [[CrossRef](#)]
6. Sorkhi, L.; Farrokhi-Rad, M.; Shahrabi, T. Electrophoretic Deposition of Hydroxyapatite–Chitosan–Titania on Stainless Steel 316 L. *Surfaces* **2019**, *2*, 458–467. [[CrossRef](#)]
7. Sikkema, R.; Baker, K.; Zhitomirsky, I. Electrophoretic deposition of polymers and proteins for biomedical applications. *Adv. Colloid Interface Sci.* **2020**, *284*, 102272. [[CrossRef](#)]
8. Chen, Y.; Ye, R.; Wang, J. Effect of voltage on the mechanical and water resistance properties of zein films by electrophoretic deposition. *Food Bioprocess Technol.* **2015**, *8*, 486–491. [[CrossRef](#)]
9. Choudhary, B.; Anwar, S.; Besra, L.; Anwar, S. Electrophoretic deposition studies of Ba (Zr-Ce-Y) O<sub>3</sub> ceramic coating. *Int. J. Appl. Ceram. Technol.* **2019**, *16*, 1022–1031. [[CrossRef](#)]
10. Dhand, C.; Singh, S.; Arya, S.K.; Datta, M.; Malhotra, B. Cholesterol biosensor based on electrophoretically deposited conducting polymer film derived from nano-structured polyaniline colloidal suspension. *Anal. Chim. Acta* **2007**, *602*, 244–251. [[CrossRef](#)]
11. Dange-Delbaere, C.; Buron, C.; Euvrard, M.; Filiâtre, C. Stability and cathodic electrophoretic deposition of polystyrene particles pre-coated with chitosan–alginate multilayer. *Colloids Surf. A Physicochem. Eng. Asp.* **2016**, *493*, 1–8. [[CrossRef](#)]
12. Biesheuvel, P.M.; Verweij, H. Theory of cast formation in electrophoretic deposition. *J. Am. Ceram. Soc.* **1999**, *82*, 1451–1455. [[CrossRef](#)]
13. De Riccardis, M.F.; Martina, V.; Carbone, D. Study of polymer particles suspensions for electrophoretic deposition. *J. Phys. Chem. B* **2013**, *117*, 1592–1599. [[CrossRef](#)] [[PubMed](#)]
14. Djošić, M.; Mišković-Stanković, V.B.; Kačarević-Popović, Z.M.; Jokić, B.M.; Bibić, N.; Mitrić, M.; Milonjić, S.K.; Jančić-Heinemann, R.; Stojanović, J. Electrochemical synthesis of nanosized monetite powder and its electrophoretic deposition on titanium. *Colloids Surf. A Physicochem. Eng. Asp.* **2009**, *341*, 110–117. [[CrossRef](#)]
15. Zhitomirsky, I.; Petric, A. Electrochemical deposition of yttrium oxide. *J. Mater. Chem.* **2000**, *10*, 1215–1218. [[CrossRef](#)]
16. Pang, X.; Zhitomirsky, I.; Niewczas, M. Cathodic electrolytic deposition of zirconia films. *Surf. Coat. Technol.* **2005**, *195*, 138–146. [[CrossRef](#)]
17. Ruwoldt, J. A Critical Review of the Physicochemical Properties of Lignosulfonates: Chemical Structure and Behavior in Aqueous Solution, at Surfaces and Interfaces. *Surfaces* **2020**, *3*, 622–648. [[CrossRef](#)]
18. Ata, M.; Liu, Y.; Zhitomirsky, I. A review of new methods of surface chemical modification, dispersion and electrophoretic deposition of metal oxide particles. *RSC Adv.* **2014**, *4*, 22716–22732. [[CrossRef](#)]
19. Ata, M.S.; Poon, R.; Syed, A.M.; Milne, J.; Zhitomirsky, I. New developments in non-covalent surface modification, dispersion and electrophoretic deposition of carbon nanotubes. *Carbon* **2018**, *130*, 584–598. [[CrossRef](#)]
20. Biswas, M.; Raichur, A.M. Electrokinetic and rheological properties of nano zirconia in the presence of rhamnolipid biosurfactant. *J. Am. Ceram. Soc.* **2008**, *91*, 3197–3201. [[CrossRef](#)]
21. Alves, A.V.; Tsianou, M.; Alexandridis, P. Fluorinated Surfactant Adsorption on Mineral Surfaces: Implications for PFAS Fate and Transport in the Environment. *Surfaces* **2020**, *3*, 516–566. [[CrossRef](#)]
22. Nawwar, M.; Poon, R.; Chen, R.; Sahu, R.P.; Puri, I.K.; Zhitomirsky, I. High areal capacitance of Fe<sub>3</sub>O<sub>4</sub>-decorated carbon nanotubes for supercapacitor electrodes. *Carbon Energy* **2019**, *1*, 124–133. [[CrossRef](#)]



23. Su, Y.; Zhitomirsky, I. Electrophoretic deposition of graphene, carbon nanotubes and composite films using methyl violet dye as a dispersing agent. *Colloids Surf. A Physicochem. Eng. Asp.* **2013**, *436*, 97–103. [[CrossRef](#)]
24. Li, J.; Zhitomirsky, I. Cathodic electrophoretic deposition of manganese dioxide films. *Colloids Surf. A Physicochem. Eng. Asp.* **2009**, *348*, 248–253. [[CrossRef](#)]
25. Ghazali, N.; Basirun, W.J.; Mohammed Nor, A.; Johan, M.R. Super-amphiphobic coating system incorporating functionalized nano- $\text{Al}_2\text{O}_3$  in polyvinylidene fluoride (PVDF) with enhanced corrosion resistance. *Coatings* **2020**, *10*, 387. [[CrossRef](#)]
26. Pornea, A.M.; Puguan, J.M.C.; Deonikar, V.G.; Kim, H. Fabrication of multifunctional wax infused porous PVDF film with switchable temperature response surface and anti corrosion property. *J. Ind. Eng. Chem.* **2020**, *82*, 211–219. [[CrossRef](#)]
27. Kim, Y.H.; Kwon, Y.S.; Shon, M.Y.; Moon, M.J. Corrosion protection performance of PVDF/PMMA-blended coatings by electrochemical impedance method. *J. Electrochem. Sci. Technol.* **2018**, *9*, 1–8. [[CrossRef](#)]
28. Ribeiro, C.; Costa, C.M.; Correia, D.M.; Nunes-Pereira, J.; Oliveira, J.; Martins, P.; Goncalves, R.; Cardoso, V.F.; Lanceros-Mendez, S. Electroactive poly (vinylidene fluoride)-based structures for advanced applications. *Nat. Protoc.* **2018**, *13*, 681. [[CrossRef](#)]
29. Ji-Hun, B.; Seung-Hwan, C. PVDF-based ferroelectric polymers and dielectric elastomers for sensor and actuator applications: A review. *Funct. Compos. Struct.* **2019**, *1*, 012003.
30. Underherbergh, J. Polyvinylidene fluoride (PVDF) appearance, general properties and processing. *Ferroelectrics* **1991**, *115*, 295–302. [[CrossRef](#)]
31. Zhong, J.; Li, W.; Qian, J.; Fu, C.; Chu, H.; Xu, J.; Ran, X.; Nie, W. Modulation of the interfacial architecture enhancing the efficiency and energy density of ferroelectric nanocomposites via the irradiation method. *J. Colloid Interface Sci.* **2021**, *586*, 30–38. [[CrossRef](#)] [[PubMed](#)]
32. Gupta, S.K.; Hernandez, C.; Zuniga, J.P.; Lozano, K.; Mao, Y. Luminescent PVDF nanocomposite films and fibers encapsulated with  $\text{La}_2\text{Hf}_2\text{O}_7$ : Eu<sup>3+</sup> nanoparticles. *SN Appl. Sci.* **2020**, *2*, 1–11. [[CrossRef](#)]
33. Wang, Y.; Zhu, X.; Zhang, T.; Bano, S.; Pan, H.; Qi, L.; Zhang, Z.; Yuan, Y. A renewable low-frequency acoustic energy harvesting noise barrier for high-speed railways using a Helmholtz resonator and a PVDF film. *Appl. Energy* **2018**, *230*, 52–61. [[CrossRef](#)]
34. Hu, P.; Yan, L.; Zhao, C.; Zhang, Y.; Niu, J. Double-layer structured PVDF nanocomposite film designed for flexible nanogenerator exhibiting enhanced piezoelectric output and mechanical property. *Compos. Sci. Technol.* **2018**, *168*, 327–335. [[CrossRef](#)]
35. Park, J.H.; Kurra, N.; AlMadhoun, M.; Odeh, I.N.; Alshareef, H.N. A two-step annealing process for enhancing the ferroelectric properties of poly (vinylidene fluoride)(PVDF) devices. *J. Mater. Chem. C* **2015**, *3*, 2366–2370. [[CrossRef](#)]
36. Foster, F.S.; Harasiewicz, K.A.; Sherar, M.D. A history of medical and biological imaging with polyvinylidene fluoride (PVDF) transducers. *IEEE Trans. Ultrason. Ferroelectr. Freq. Control* **2000**, *47*, 1363–1371. [[CrossRef](#)]
37. Kang, G.-d.; Cao, Y.-m. Application and modification of poly (vinylidene fluoride)(PVDF) membranes—A review. *J. Membr. Sci.* **2014**, *463*, 145–165. [[CrossRef](#)]
38. Barbosa, J.C.; Correia, D.M.; Gonçalves, R.; de Zea Bermudez, V.; Silva, M.M.; Lanceros-Mendez, S.; Costa, C.M. Enhanced ionic conductivity in poly(vinylidene fluoride) electrospun separator membranes blended with different ionic liquids for lithium ion batteries. *J. Colloid Interface Sci.* **2021**, *582*, 376–386. [[CrossRef](#)]
39. Cui, Y.; Yang, L.; Zheng, J.; Wang, Z.; Li, B.; Yan, Y.; Meng, M. Synergistic interaction of Z-scheme 2D/3D g- $\text{C}_3\text{N}_4$ /BiOI heterojunction and porous PVDF membrane for greatly improving the photodegradation efficiency of tetracycline. *J. Colloid Interface Sci.* **2021**, *586*, 335–348. [[CrossRef](#)]
40. Wei, N.; Li, Z.; Li, Q.; Yang, E.; Xu, R.; Song, X.; Sun, J.; Dou, C.; Tian, J.; Cui, H. Scalable and low-cost fabrication of hydrophobic PVDF/WS2 porous membrane for highly efficient solar steam generation. *J. Colloid Interface Sci.* **2021**, *588*, 369–377. [[CrossRef](#)]
41. Zhao, B.; Hu, J.; Ren, W.; Xu, F.; Wu, X.; Shi, P.; Ye, Z.-G. A new biosensor based on PVDF film for detection of nucleic acids. *Ceram. Int.* **2015**, *41*, S602–S606. [[CrossRef](#)]
42. Song, Y.-S.; Yun, Y.; Lee, D.Y.; Kim, B.-Y. Effect of PVDF Concentration and Number of Fiber Lines on Piezoelectric Properties of Polymeric PVDF Biosensors. *Fibers Polym.* **2021**, *22*, 1200–1207. [[CrossRef](#)]
43. Hartono, A.; Sanjaya, E.; Ramli, R. Glucose sensing using capacitive biosensor based on polyvinylidene fluoride thin film. *Biosensors* **2018**, *8*, 12. [[CrossRef](#)]
44. Häsler, E.; Stein, L.; Harbauer, G. Implantable physiological power supply with PVDF film. *Ferroelectrics* **1984**, *60*, 277–282. [[CrossRef](#)]
45. Yu, Y.; Sun, H.; Orbay, H.; Chen, F.; England, C.G.; Cai, W.; Wang, X. Biocompatibility and in vivo operation of implantable mesoporous PVDF-based nanogenerators. *Nano Energy* **2016**, *27*, 275–281. [[CrossRef](#)] [[PubMed](#)]
46. Lu, L.; Ding, W.; Liu, J.; Yang, B. Flexible PVDF based piezoelectric nanogenerators. *Nano Energy* **2020**, *78*, 105251. [[CrossRef](#)]
47. Houis, S.; Engelhardt, E.; Wurm, F.; Gries, T. Application of polyvinylidene fluoride (PVDF) as a biomaterial in medical textiles. In *Medical and Healthcare Textiles*; Elsevier: Amsterdam, The Netherlands, 2010; pp. 342–352.
48. Wang, H.; Klosterhalfen, B.; Müllen, A.; Otto, T.; Dievernich, A.; Jockenhövel, S. Degradation resistance of PVDF mesh in vivo in comparison to PP mesh. *J. Mech. Behav. Biomed. Mater.* **2021**, *119*, 104490. [[CrossRef](#)]
49. Haddadi, S.A.; Ghaderi, S.; Amini, M.; Ramazani, S.A. Mechanical and piezoelectric characterizations of electrospun PVDF-nanosilica fibrous scaffolds for biomedical applications. *Mater. Today Proc.* **2018**, *5*, 15710–15716. [[CrossRef](#)]
50. Kyeremateng, N.A.; Gukte, D.; Ferch, M.; Buk, J.; Hrebicek, T.; Hahn, R. Preparation of a Self-Supported  $\text{SiO}_2$  Membrane as a Separator for Lithium-Ion Batteries. *Batter. Supercaps* **2020**, *3*, 456–462. [[CrossRef](#)]

51. Prasanna, K.; Subburaj, T.; Jo, Y.N.; Lee, C.W. Optimization of electrophoretic suspension to fabricate  $\text{Li}[\text{Ni}_{1/3}\text{Co}_{1/3}\text{Mn}_{1/3}]\text{O}_2$  based positive electrode for Li-ion batteries. *Electrochim. Acta* **2013**, *95*, 295–300. [[CrossRef](#)]
52. Hagberg, J.; Maples, H.A.; Alvim, K.S.; Xu, J.; Johannisson, W.; Bismarck, A.; Zenkert, D.; Lindbergh, G. Lithium iron phosphate coated carbon fiber electrodes for structural lithium ion batteries. *Compos. Sci. Technol.* **2018**, *162*, 235–243. [[CrossRef](#)]
53. Ui, K.; OKURA, K.; Koura, N.; Tsumeda, S.; Tamamitsu, K. Fabrication of the electrode for capacitor cell prepared by the electrophoretic deposition method. *Electrochemistry* **2007**, *75*, 604–606. [[CrossRef](#)]
54. Lau, K.T.; Suan, M.S.M.; Zaimi, M.; Abd Razak, J.; Azam, M.; Mohamad, N. Microstructure and Phase of Poly (Vinylidene Fluoride) Films by Electrophoretic Deposition: Effect of Polymer Dispersion's Stirring Conditions. *J. Adv. Manuf. Technol. (JAMT)* **2016**, *10*, 57–66.
55. Lau, K.T.; Ab Razak, M.H.R.; Kok, S.L.; Zaimi, M.; Abd Rashid, M.W.; Mohamad, N.; Azam, M.A. Electrophoretic Deposition and Heat Treatment of Steel-Supported PVDF-Graphite Composite Film. In *Applied Mechanics and Materials*; Trans Tech Publications: Zurich, Switzerland, 2015; pp. 412–416.
56. Yin, J.; Fukui, T.; Murata, K.; Matsuda, M.; Miyake, M.; Hirabayashi, T.; Yamamuro, S. Fabrication of protective KB/PVdF composite films on stainless steel substrates for PEFCs through electrophoretic deposition. *J. Ceram. Soc. Jpn.* **2008**, *116*, 201–204. [[CrossRef](#)]
57. Zhao, Q.; Veldhuis, S.; Mathews, R.; Zhitomirsky, I. Influence of chemical structure of bile acid dispersants on electrophoretic deposition of poly (vinylidene fluoride) and composites. *Colloids Surf. A Physicochem. Eng. Asp.* **2021**, *627*, 127181. [[CrossRef](#)]
58. Hashiba, M.; Okamoto, H.; Nurishi, Y.; Hiramatsu, K. The zeta-potential measurement for concentrated aqueous suspension by improved electrophoretic mass transport apparatus—application to  $\text{Al}_2\text{O}_3$ ,  $\text{ZrO}_3$  and SiC suspensions. *J. Mater. Sci.* **1988**, *23*, 2893–2896. [[CrossRef](#)]
59. Lee, B.P.; Messersmith, P.B.; Israelachvili, J.N.; Waite, J.H. Mussel-inspired adhesives and coatings. *Annu. Rev. Mater. Res.* **2011**, *41*, 99–132. [[CrossRef](#)]
60. Lee, H.; Lee, B.P.; Messersmith, P.B. A reversible wet/dry adhesive inspired by mussels and geckos. *Nature* **2007**, *448*, 338–341. [[CrossRef](#)]
61. Xu, N.; Li, Y.; Zheng, T.; Xiao, L.; Liu, Y.; Chen, S.; Zhang, D. A mussel-inspired strategy for CNT/carbon fiber reinforced epoxy composite by hierarchical surface modification. *Colloids Surf. A Physicochem. Eng. Asp.* **2022**, *635*, 128085. [[CrossRef](#)]
62. Sun, Y.; Ata, M.; Zhitomirsky, I. Electrophoretic deposition of  $\text{TiO}_2$  nanoparticles using organic dyes. *J. Colloid Interface Sci.* **2012**, *369*, 395–401. [[CrossRef](#)]
63. Sun, Y.; Zhitomirsky, I. Electrophoretic deposition of titanium dioxide using organic acids as charging additives. *Mater. Lett.* **2012**, *73*, 190–193. [[CrossRef](#)]
64. Sun, Y.; Wang, Y.; Zhitomirsky, I. Dispersing agents for electrophoretic deposition of  $\text{TiO}_2$  and  $\text{TiO}_2$ -carbon nanotube composites. *Colloids Surf. A Physicochem. Eng. Asp.* **2013**, *418*, 131–138. [[CrossRef](#)]
65. Ata, M.; Zhitomirsky, I. Preparation of  $\text{MnO}_2$  and composites for ultracapacitors. *Mater. Manuf. Processes* **2013**, *28*, 1014–1018.
66. Wu, K.; Wang, Y.; Zhitomirsky, I. Electrophoretic deposition of  $\text{TiO}_2$  and composite  $\text{TiO}_2$ - $\text{MnO}_2$  films using benzoic acid and phenolic molecules as charging additives. *J. Colloid Interface Sci.* **2010**, *352*, 371–378. [[CrossRef](#)] [[PubMed](#)]
67. Wang, Y.; Zhitomirsky, I. Bio-inspired catechol chemistry for electrophoretic nanotechnology of oxide films. *J. Colloid Interface Sci.* **2012**, *380*, 8–15. [[CrossRef](#)]
68. Sharma, T.; Je, S.-S.; Gill, B.; Zhang, J.X. Patterning piezoelectric thin film PVDF-TrFE based pressure sensor for catheter application. *Sens. Actuators A Phys.* **2012**, *177*, 87–92. [[CrossRef](#)]
69. Bhatt, A.S.; Bhat, D.K.; Santosh, M. Crystallinity, conductivity, and magnetic properties of PVDF- $\text{Fe}_3\text{O}_4$  composite films. *J. Appl. Polym. Sci.* **2011**, *119*, 968–972. [[CrossRef](#)]
70. Venevtsev, Y.N.; Gagulin, V.V.; Zhitomirsky, I.D. Material science aspects of seignette-magnetism problem. *Ferroelectrics* **1987**, *73*, 221–248. [[CrossRef](#)]
71. Luo, H.; Hanagud, S. PVDF film sensor and its applications in damage detection. *J. Aerosp. Eng.* **1999**, *12*, 23–30. [[CrossRef](#)]
72. Li, W.; Song, Z.; Zhong, J.; Qian, J.; Tan, Z.; Wu, X.; Chu, H.; Nie, W.; Ran, X. Multilayer-structured transparent MXene/PVDF film with excellent dielectric and energy storage performance. *J. Mater. Chem. C* **2019**, *7*, 10371–10378. [[CrossRef](#)]
73. Kobayashi, M.; Tashiro, K.; Tadokoro, H. Molecular vibrations of three crystal forms of poly (vinylidene fluoride). *Macromolecules* **1975**, *8*, 158–171. [[CrossRef](#)]
74. Zeng, Z.; Yu, D.; He, Z.; Liu, J.; Xiao, F.-X.; Zhang, Y.; Wang, R.; Bhattacharyya, D.; Tan, T.T.Y. Graphene oxide quantum dots covalently functionalized PVDF membrane with significantly-enhanced bactericidal and antibiofouling performances. *Sci. Rep.* **2016**, *6*, 20142. [[CrossRef](#)] [[PubMed](#)]